PAPER *Special Issue on Personal, Indoor and Mobile Radio Communications*

Proposal of Higher-Order Spread Spectrum Direct Optical Switching CDMA System

Kazuo KUMAMOTO†, ***Student Member***, **Katsutoshi TSUKAMOTO**†, ***and*** **Shozo KOMAKI**†, ***Regular Members***

SUMMARY This paper proposes higher-order spread spectrum direct optical switching CDMA system and an aliasing canceler to remove the aliasing distortion caused by higher-order bandpass sampling. Theoretical analysis of the signal quality shows that the 3rd order bandpass sampling scheme can improve the carrier-to-interference-power ratio compared with the conventional 1st order bandpass sampling scheme, by 5 dB.

key words: *microwave photonics, radio-over-fiber system, optical CDMA, higher-order sampling, spectral aliasing*

1. Introduction

Recently, radio-over-fiber systems and radio highway networks have been studied to solve many problems in the microcell/picocell technologies [1], [2]. Figure 1 illustrates the concept of radio highways, which can realize the universal capability and flexibility for various types of air interfaces. A radio base station (RBS) is only equipped with an E/O (electric-to-optic) and O/E (optic-to-electric) converters, and all of complicated functions such as RF modulation, demodulation and so on, are performed at a control station (CS).

As a multiple access method in radio highways, CDMA will be a strong candidate, because CDMA is superior to TDMA [3] in its asynchronous access property, and to SCMA [4] in its flexibility and transparency for radio air interfaces. Time-spreading CDMA [5], [6], spectral encoding CDMA [7] and optical coherent coding (CC)-CDMA systems [8] are available to multiplex radio signals in radio highways. However, in the time-spreading CDMA using fiber delay lines, the encoding and decoding are performed by delayed optical pulses in time domain, thus this method is rigid to the code assignment. The spectral encoding CDMA requires many laser sources, thus it is difficult to configure the encoder and decoder. Furthermore, in the optical CC-CDMA, the code correlation is provided by optical heterodyne detection or optical phase detection, but the optical heterodyne detection is very complicated, and the optical phase detection needs some narrowband optical filters that are very sensitive to temperature changes.

On the other hand, we have proposed direct optical switching (DOS)-CDMA systems [9], [10], which can easily encode and decode an optical signal with an optical switch (OSW). Furthermore, any types of radio signals can be converted into CDMA signals, so the optical direct detection can be employed. In the DOS-CDMA system in Refs. [9], [10], when a radio signal is transmitted by bandpass sampling, its spreading code period is identical to the required period determined by the bandpass sampling theorem in order not to generate any distortion caused by the spectral aliasing.

For the DOS-CDMA systems, the following two methods are possible to improve the received carrier-to-interference-power ratio (CIR). The first method is to increase a chip rate of the spreading code to expand its code length within the required bandpass sampling period. The high chip rate can be realized by a high speed OSW. Up to now, this first method has been considered for the CIR improvement in Refs. [9], [10]. On the other hand, the second method is an expansion of code period* in time domain with its chip rate kept. We have found this novel method from the higher-order sampling theorem [11], and it can be combined with the first method to obtain higher CIR. However, the problem in the second method is a spectral aliasing distortion of the spread spectrum signal.

In this paper, we newly propose the higher-order spread spectrum direct optical switching CDMA system based on the second method to obtain CIR im-

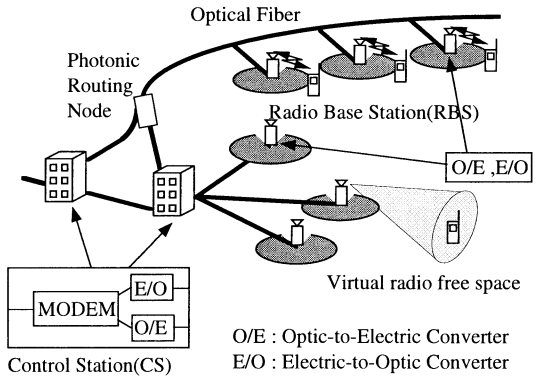

Fig. 1 Concept of the fiber-optic radio highway.

Manuscript received December 10, 1999.
Manuscript revised March 18, 2000.

†The authors are with the Department of Communications Eng., Faculty of Eng., Osaka University, Suita-shi, 565-0871 Japan.

*In this paper, we call the number of chips in a code word "code length," and the time length of a code is called "code period."

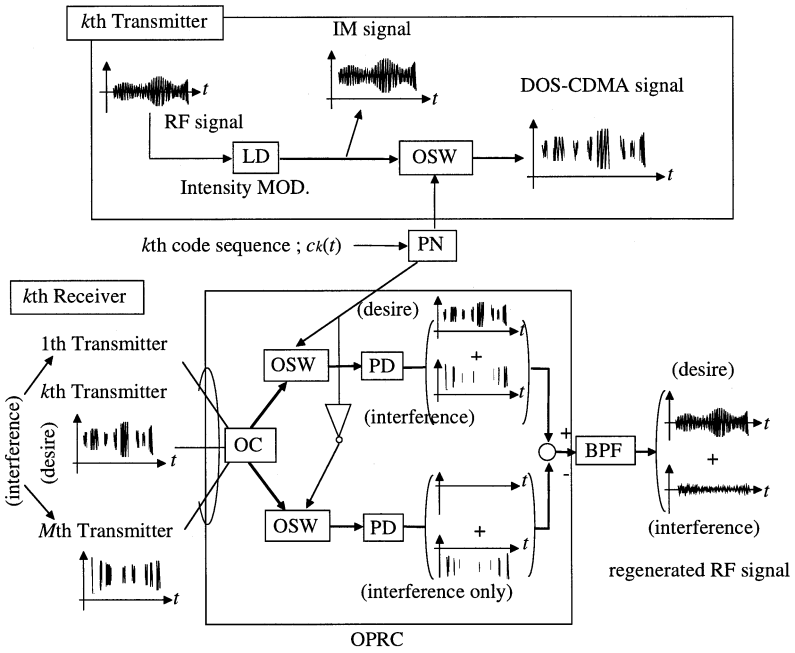

Fig. 2 Configuration of the DOS-CDMA system.

provement. To eliminate spectral aliasing distortions caused by the higher-order spectrum spreading [11], we also propose a new type of aliasing canceler [12], [13]. We theoretically analyze the CIR of radio signals at the receiver, and examine CIR improvement. To realize the proposal aliasing canceler, moreover, we attempt to construct it with transversal filters, and investigate its irreducible distortion by computer simulations.

We describe the principle of DOS-CDMA radio highway network in Sect. 2, and we propose the higher-order spread spectrum DOS-CDMA system and the aliasing canceler in Sect. 3. Next, in Sect. 4, we theoretically analyze the carrier-to-interference-plus-noise-power ratio (CINR) of the regenerated radio signals at the CS. Finally, in Sect. 5, we will discuss the construction method and the performance of the proposed aliasing canceler.

2. DOS-CDMA System and Its Improving Method of CIR

2.1 Principle of DOS-CDMA System

Figure 2 illustrates the configuration of the DOS-CDMA system [9], [10]. At the transmitter of k-th RBS, an optical carrier is intensity-modulated (IM) by the RF signal received at the RBS, and on-off-encoded at the OSW driven with the k-th biased bipolar code, $c_k(t)$. After that, many DOS-CDMA signals from M transmitters are multiplexed, and transferred to the CS. At the CS, DOS-CDMA signals are power-split to each receiver, and correlated at the optical polarity reversing correlator (OPRC) [9] driven with the biased bipolar code identical to a desired transmitter. At the OPRC, the DOS-CDMA signal is divided into two branches by 3 dB coupler. The OSW of the upper branch is driven with "1" of the biased bipolar code and the OSW of the lower branch is driven with "0" of the biased bipolar code. As a result, the PD output of the upper branch is the sum of the desired signal and the interference signals, and the PD output of the other branch includes only the interference signals. The power of the interference signals from both branches can be reduced by the subtraction after photodetections. Thus, as the output of OPRC, we obtain the desired signal contaminated with some reduced-power interference signals. At this stage, however, the desired signal is still the on-off pulsed signal, so in order to obtain the original RF signal, we finally interpolate it by using a bandpass filter (BPF).

2.2 CIR Improvement Method for DOS-CDMA System

2.2.1 Conventional Method by Using High Chip Rate Code

The on-off switching at the transmitter in DOS-CDMA system corresponds to the bandpass natural sampling of RF signals [9], [10]. Let T_L, T_C and L denote the code period, the chip width and the code length of a spreading code, respectively. Thus, to interpolate a DOS-CDMA signal at the BPF without any distortion, the code period, T_L, has to be set shorter than the required maximal sampling period, T_S, [9], [10]. Because the minimal sampling rate of natural bandpass sam-

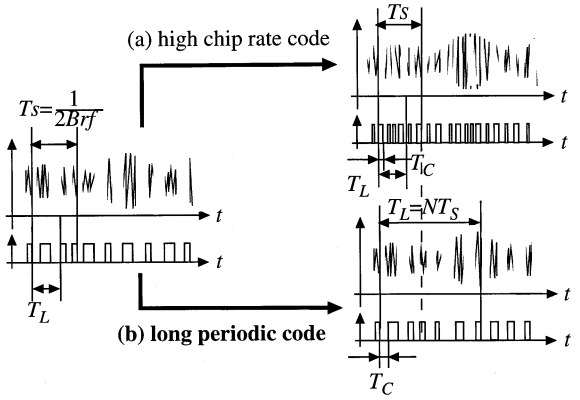

Fig. 3 Two methods to improve CIR.

pling, $1/T_S$, is to be twice the radio signal bandwidth, B_{rf}. The code period, T_L, should have the following property;

$$T_L = LT_C \leq T_S = \frac{1}{2B_{rf}}. \tag{1}$$

In this case, signal encoding is performed within T_S, and the CIR can be improved by increasing the chip rate, $1/T_C$, as illustrated in Fig. 3(a).

2.2.2 Proposed Method by Using Long Periodic Code

The CIR of the DOS-CDMA system is given by

$$\begin{cases} CIR_p = \dfrac{L}{0.29(M-1)} & \text{for prime codes} \\ CIR_M = \dfrac{L}{M-1} & \text{for M sequences} \end{cases} \tag{2}$$

where M is the number of connected RBS [9], [10]. It is seen from Eq. (2) that the CIR is almost in proportion to the code length L, that is in inverse proportion to the cross correlation value of the spreading code, and it is independent of the chip rate, $1/T_C$. This means that we can improve CIR by using a longer periodic code as illustrated in Fig. 3(b).

By the way, the on-off switching with a spreading code corresponds to the bandpass sampling with a random-positioned pulse sequence. In the case of using a code with its code period, T_L, set to be longer than T_S, the spread signal can be regarded as a higher-order bandpass sampled signal [11]. Therefore, when we expand the code length, L, with its chip rate fixed in order to improve CIR, the average pulse interval must be shorter than the required maximal sampling period, $T_S = 1/2B_{rf}$ [11]. In the Nth order bandpass sampling, this condition can be written as

$$\frac{T_L}{n_p} = \frac{NT_S}{n_p} \leq T_S = \frac{1}{2B_{rf}}, \tag{3}$$

where n_p represents the number of "1" in the Nth order expanded code. Figure 4 shows the upper bound of CIR improvement in this method for the case of using a prime code with its L of 97^2. The CIR can be improved as the sampling order, N, increases, but in the region of N of more than 100, no further improvement can be obtained. This is because the average pulse interval exceeds T_S.

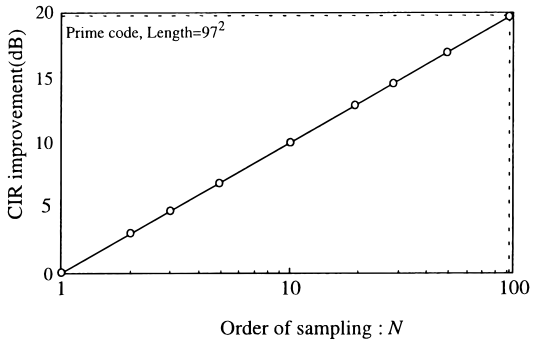

Fig. 4 Upper bound of proposed scheme.

The results shown in Fig. 4 show ideal improvements when ignoring the intrinsic distortions in the higher-order sampling. The received signal is distorted by spectral aliasing in the Nth order bandpass sampling. In the next section, we discuss the canceler for this aliasing distortion, and propose the higher-order spread spectrum DOS-CDMA system.

3. Higher-Order Spread Spectrum DOS-CDMA System

In the first part of this section, we propose an aliasing canceler for higher-order spread spectrum DOS-CDMA system, and next we describe the overall configuration of the proposed system.

3.1 Aliasing Cancelation in Higher-Order Bandpass Sampling

Figure 5 illustrates the 1st order and the Nth order bandpass natural sampling process of the signal. In the Nth order bandpass sampling, the sampling pulses of a code sequence are randomly positioned in a period of $T_{L_N} = NT_S$.

A sampled signal, $\hat{f}(t)$, is expressed as

$$\hat{f}(t) = \sum_{i=1}^{N} f_i(t) = \sum_{i=1}^{N} \left\{ f(t) \times \sum_{n=-\infty}^{+\infty} [p(t - nT_{L_N} - \tau_i)] \right\} \quad (i = 1, 2, 3, \cdots, N), \tag{4}$$

where $f(t)$, $f_i(t)$, $p(t)$ and τ_i are the received RF signal which intensity modulates LD, the i-th sampled sequence, the rectangular pulse with its width of T_C and its amplitude of 1, and the time position of the i-th pulse, respectively. The spectrum of the Nth order bandpass sampled signal, $\hat{F}(f)$, is given by

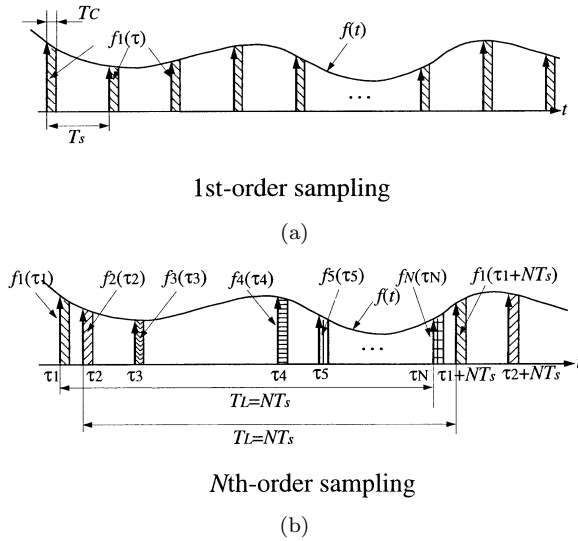

Fig. 5 Bandpass natural sampling process of the 1st order and the Nth order.

$$\hat{F}(f) = \sum_{i=1}^{N} F_i(f) \quad (i = 1, 2, 3, \cdots, N) \tag{5}$$

and

$$F_i(f) = \sum_{n=-\infty}^{+\infty} \frac{T_C}{T_{L_N}} \frac{\sin \pi n \frac{T_C}{T_{L_N}}}{\pi n \frac{T_C}{T_{L_N}}} F\left(f - \frac{n}{T_{L_N}}\right) e^{-j2\pi n \tau_i / T_{L_N}} \quad (i = 1, 2, 3, \cdots, N) \tag{6}$$

It is seen from Eq. (4) that $\hat{f}(t)$ is a summation of mutually independent N sampled sequences, $f_1(t), f_2(t), \cdots$, and $f_N(t)$. We can regenerate the RF signal from each of N sequences, $f_i(t)$ $(i = 1, 2, \cdots, N)$, by using interpolation at a bandpass-filtering. A spectral aliasing causes the distortion in the RF signal regenerated from one sequence, $f_i(t)$, because the sampling period of $f_i(t)$, T_{L_N}, is NT_S which is longer than the required maximal period, T_S. When bandpass-filtering each of N sampled sequences, $f_i(t)$ $(i = 1, 2, \cdots, N)$, and summing them, however, the appropriate amplitude and phase characteristics of N filters can make it possible to regenerate only the desired RF signal and eliminate aliasing components [11]. We call this filterbank "aliasing canceler." In the following description, we derive the required characteristics of N filters.

Let $H_i(f)$ $(i = 1, 2, \cdots, N)$ denotes the transfer function of these N filters. Each of N sampled sequence, $f_i(t)$ $(i = 1, 2, \cdots, N)$, should be passed through a different filter, $H_i(f)$ $(i = 1, 2, \cdots, N)$, to introduce a different gain and phase shift. Therefore, we have to divide $\hat{f}(t)$ into each $f_i(t)$ by the use of a switch before filtering.

In the Nth order bandpass sampling, the interpolation of signal is performed in N BPFs with characteristics of, $H_i(f)$ $(i = 1, 2, \cdots, N)$. The required $H_i(f)$ of N filters can be derived by solving the equation [11]

$$\sum_{i=1}^{N} H_i(f) F_i(f) = F(f). \tag{7}$$

It is very difficult to derive general solutions $H_i(f)$ $(i = 1, 2, \cdots, N)$ from Eq. (7). So, for the sake of simple discussion, we first derive transfer functions in the case of 3rd order bandpass sampling.

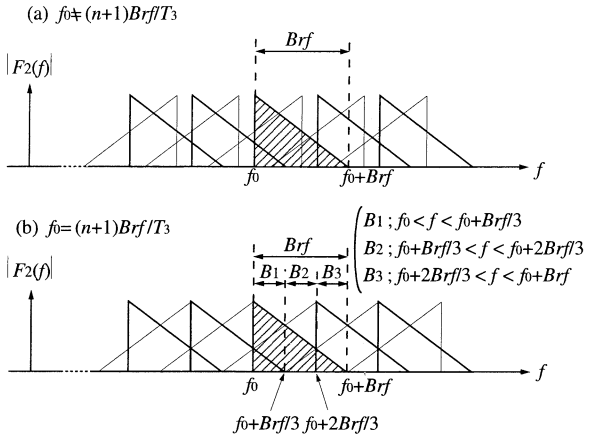

Fig. 6 Spectrum of the 3rd order sampled signal when sampling period, T_{L_3}, is $3T_S$.

Figure 6 illustrates the spectrum of $f_2(f)$, $F_2(f)$, in the case that the 3rd order bandpass sampling period, T_{L_3}, is $3T_S$. The state of spectral aliasing depends on the carrier frequency, f_0, and the bandwidth, B_{rf}, of the sampled RF signal. In this figure, the spectrum with shadow represents the desired spectrum, and the spectrum with bold lines represents the aliasing spectrum generating in the positive frequency band, and the spectrum with slim lines represents the aliasing spectrum generating in the negative frequency band. In the case of $f_0 \neq (n+1)B_{rf}/T_{L_3}$ (n: integer) (Fig. 6(a)), three spectral aliasings appear in the same frequency band, and in such case, we can not remove aliasing distortion [11].

On the other hand, in the case of $f_0 = (n+1)B_{rf}/T_{L_3}$ (n: integer) (Fig. 6(b)), two spectral aliasings appear at any band in signal frequency band $(f_0, f_0 + B_{rf})$ at most. This means that we can solve Eq. (7) for $N = 3$, and derive $H_i(f)$ $(i = 1, 2, 3)$ in order to remove aliasing components, under the condition that the radio frequency, f_0, is

$$f_0 = (n+1)\frac{B_{rf}}{T_{L_3}}. \tag{8}$$

It is found from Fig. 6(b) that the state of spectral aliasing in three different frequency bands are different from each other. Thus Eq. (7) must be solved for each of three bands,

$$\begin{cases} B_1; f_0 < f < f_0 + \dfrac{B_{rf}}{3} \\ B_2; f_0 + \dfrac{B_{rf}}{3} < f < f_0 + \dfrac{2B_{rf}}{3} \\ B_3; f_0 + \dfrac{2B_{rf}}{3} < f < f_0 + B_{rf} \end{cases} \cdot \tag{9}$$

For the first frequency band, $B_1(f_0 < f < f_0 + B_{rf}/3)$, Eq. (7) yields

$$\begin{cases} H_1(f) + H_2(f) + H_3(f) = 2B_{rf}T_{L_3} \\ H_1(f) + e^{j2\pi(\tau_2-\tau_1)/T_{L_3}} H_2(f) \\ \quad + e^{j2\pi(\tau_3-\tau_1)/T_{L_3}} H_3(f) = 0 \\ H_1(f) + e^{-j2\pi l(\tau_2-\tau_1)/T_{L_3}} H_2(f) \\ \quad + e^{-j2\pi l(\tau_3-\tau_1)/T_{L_3}} H_3(f) = 0 \end{cases}$$

$$\left(B_1; f_0 < f < f_0 + \frac{B_{rf}}{3}\right) \tag{10}$$

First equation is needed for the desired component, and two left equations show the cancelation of aliasing components. For the second frequency band, $B_2; (f_0 + B_{rf}/3 < f < f_0 + 2B_{rf}/3)$, and the third band, $B_3; (f_0 + 2B_{rf}/3 < f < f_0 + B_{rf})$, Eq. (7) gives the following equations, respectively:

$$\begin{cases} H_1(f) + H_2(f) + H_3(f) = 2B_{rf}T_{L_3} \\ H_1(f) + e^{-j2\pi l(\tau_2-\tau_1)/T_{L_3}} H_2(f) \\ \quad + e^{-j2\pi l(\tau_3-\tau_1)/T_{L_3}} H_3(f) = 0 \\ H_1(f) + e^{-j2\pi(l+1)(\tau_2-\tau_1)/T_{L_3}} H_2(f) \\ \quad + e^{-j2\pi(l+1)(\tau_3-\tau_1)/T_{L_3}} H_3(f) = 0 \end{cases}$$

$$\left(B_2; f_0 + \frac{B_{rf}}{3} < f < f_0 + \frac{2B_{rf}}{3}\right) \tag{11}$$

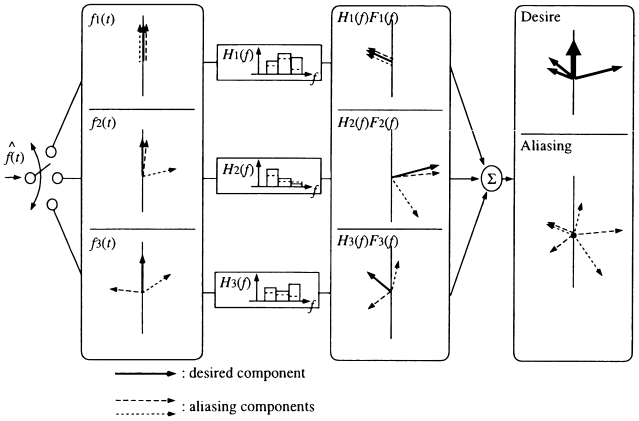

Fig. 7 Configuration of the aliasing canceler and the operation of spectral aliasing removal.

and

$$\begin{cases} H_1(f) + H_2(f) + H_3(f) = 2B_{rf}T_{L_3} \\ H_1(f) + e^{-j2\pi(\tau_2-\tau_1)/T_{L_3}} H_2(f) \\ \quad + e^{-j2\pi(\tau_3-\tau_1)/T_{L_3}} H_3(f) = 0 \\ H_1(f) + e^{-j2\pi l(\tau_2-\tau_1)/T_{L_3}} H_2(f) \\ \quad + e^{-j2\pi l(\tau_3-\tau_1)/T_{L_3}} H_3(f) = 0 \end{cases}$$

$$\left(B_3; f_0 + \frac{2B_{rf}}{3} < f < f_0 + B_{rf}\right) \tag{12}$$

Assuming $\tau_1 = 0$ without any loss of generality, $H_1(f), H_2(f)$ and $H_3(f)$ can be derived from Eqs. (10)–(12), as Eqs. (13)–(15).

Where $\phi(x) = e^{j2\pi x/T_{L_3}}$. It is seen from Eqs. (13)–(15) that the amplitude and phase characteristics of $H_i(f)$ $(i = 1, 2, 3)$ are fixed in each band of B_1, B_2 and B_3.

Figure 7 illustrates the configuration of the aliasing canceler and the operation of spectral aliasing removal

$$H_1(f) = \begin{cases} \dfrac{2B_{rf}T_{L_3}\{\phi(\tau_2 - l\tau_3) - \phi(l\tau_2 - \tau_3)\}}{\phi(\tau_2 - l\tau_3) - \phi(l\tau_2 - \tau_3) + \phi(\tau_3) - \phi(l\tau_3) + \phi(l\tau_2) - \phi(\tau_2)} \\ \quad \left(B_1; f_0 < f < f_0 + \dfrac{B_{rf}}{3}\right) \\ \dfrac{2B_{rf}T_{L_3}\{\phi(-l\tau_2 - (l+1)\tau_3) - \phi((l+1)\tau_2 + l\tau_3)\}}{\phi(-l\tau_2 - (l+1)\tau_3) - \phi((l+1)\tau_2 - l\tau_3) + \phi(-l\tau_3) - \phi((l+1)\tau_3) + \phi((l+1)\tau_2) - \phi(-l\tau_2)} \\ \quad \left(B_2; f_0 + \dfrac{B_{rf}}{3} < f < f_0 + \dfrac{2B_{rf}}{3}\right) \\ \dfrac{2B_{rf}T_{L_3}\{\phi(\tau_2) - \phi(-l\tau_2)\}}{\phi(-l\tau_2 - \tau_3) - \phi(\tau_2 + l\tau_3) + \phi(-l\tau_3) - \phi(\tau_3) + \phi(\tau_2) - \phi(-l\tau_2)} \\ \quad \left(B_3; f_0 + \dfrac{2B_{rf}}{3} < f < f_0 + B_{rf}\right) \\ 0 \quad \text{(elsewhere)} \end{cases} \tag{13}$$

$$H_2(f)=\begin{cases}\dfrac{2B_{rf}T_{L_3}\{\phi(\tau_3)-\phi(l\tau_3)\}}{\phi(\tau_2-l\tau_3)-\phi(l\tau_2-\tau_3)+\phi(\tau_3)-\phi(l\tau_3)+\phi(l\tau_2)-\phi(\tau_2)} \\ \quad \left(B_1; f_0<f<f_0+\dfrac{B_{rf}}{3}\right) \\ \dfrac{2B_{rf}T_{L_3}\{\phi(-l\tau_3)-\phi((l+1)\tau_3)\}}{\phi(-l\tau_2-(l+1)\tau_3)-\phi((l+1)\tau_2+l\tau_3)+\phi(-l\tau_3)-\phi((l+1)\tau_3)+\phi((l+1)\tau_2)-\phi(-l\tau_2)} \\ \quad \left(B_2; f_0+\dfrac{B_{rf}}{3}<f<f_0+\dfrac{2B_{rf}}{3}\right) \\ \dfrac{2B_{rf}T_{L_3}\{\phi(-l\tau_3)-\phi(\tau_3)\}}{\phi(-l\tau_2-\tau_3)-\phi(\tau_2+l\tau_3)+\phi(-l\tau_3)-\phi(\tau_3)+\phi(\tau_2)-\phi(-l\tau_2)} \\ \quad \left(B_3; f_0+\dfrac{2B_{rf}}{3}<f<f_0+B_{rf}\right) \\ 0 \quad \text{(elsewhere)}\end{cases} \tag{14}$$

$$H_3(f)=\begin{cases}\dfrac{2B_{rf}T_{L_3}\{\phi(l\tau_2)-\phi(\tau_2)\}}{\phi(\tau_2-l\tau_3)-\phi(l\tau_2-\tau_3)+\phi(\tau_3)-\phi(l\tau_3)+\phi(l\tau_2)-\phi(\tau_2)} \\ \quad \left(B_1; f_0<f<f_0+\dfrac{B_{rf}}{3}\right) \\ \dfrac{2B_{rf}T_{L_3}\{\phi((l+1)\tau_2)-\phi(-l\tau_2)\}}{\phi(-l\tau_2-(l+1)\tau_3)-\phi((l+1)\tau_2+l\tau_3)+\phi(-l\tau_3)-\phi((l+1)\tau_3)+\phi((l+1)\tau_2)-\phi(-l\tau_2)} \\ \quad \left(B_2; f_0+\dfrac{B_{rf}}{3}<f<f_0+\dfrac{2B_{rf}}{3}\right) \\ \dfrac{2B_{rf}T_{L_3}\{\phi(\tau_2)-\phi(-l\tau_2)\}}{\phi(-l\tau_2-\tau_3)-\phi(\tau_2+l\tau_3)+\phi(-l\tau_3)-\phi(\tau_3)+\phi(\tau_2)-\phi(-l\tau_2)} \\ \quad \left(B_3; f_0+\dfrac{2B_{rf}}{3}<f<f_0+B_{rf}\right) \\ 0 \quad \text{(elsewhere)}\end{cases} \tag{15}$$

for the 3rd order bandpass sampling. The aliasing canceler is configured with an electrical switch, three BPFs ($H_1(f), H_2(f)$ and $H_3(f)$), and a combiner at the output stage. Input of the aliasing canceler is the 3rd order sampled signal, $\hat{f}(t)$, and they are divided into each pulse, $f_i(t)$ $(i=1,2,3)$ at the switch with its switching speed of the chip rate, $1/T_C$. In Fig. 7, the vector description of $f_i(t)$ $(i=1,2,3)$ illustrates the aliasing canceling operation. The sum of three desired components from the $f_i(t)$ $(i=1,2,3)$ represented by the real line vector becomes the original RF signal, $f(t)$, after passing the BPFs ($H_1(f), H_2(f)$ and $H_3(f)$). On the other hand, each of aliasing components in the $f_i(t)$ $(i=1,2,3)$ are independently gained and phase-rotated at BPFs ($H_1(f), H_2(f)$ and $H_3(f)$) and canceled out after the combination.

Any N filters for Nth order bandpass sampling can be derived by using the same method as the 3rd order case without any loss of generality. In the Nth order bandpass sampling case, the condition to remove aliasing components is given by

$$f_0=(n+1)\frac{B_{rf}}{T_{L_N}}=(n+1)\frac{B_{rf}}{NT_S} \quad (n\text{: integer}) \tag{16}$$

and the state of spectral aliasing in the different N frequency bands are different from each other, so N BPFs are needed in order to remove $N-1$ of spectral aliasing. However, as the order N increases, the configuration of aliasing canceler will be rather complicated. From the view point of realization, the 3rd order bandpass sampling and the corresponding aliasing canceler is important to be discussed, because of a fine CIR improvement of 5 dB as shown in Fig. 4. So, in this paper, the discussion and the performance analysis will be focused on the case of the proposed system using the 3rd order bandpass sampling.

3.2 System Configuration

Figure 8 illustrates a configuration of the proposed

higher-order spread spectrum DOS-CDMA system. At the transmitter of RBS, the optical intensity-modulating (IM) signal is higher-order sampled at OSW. At the k-th receiver, the received signal is on-off switched by a long periodic code identical with the k-th RBS. The output of OPRC is the k-th higher-order sampled signal contaminated with suppressed interference signals. The desired k-th sampled signal becomes the original k-th RF signal after passing through the aliasing canceler proposed in the previous Sect. 3.1. On the other hand, the interference power within the frequency band of the RF signal does not change at the output of the aliasing canceler. This fact will be explained in the following Sect. 4.1.

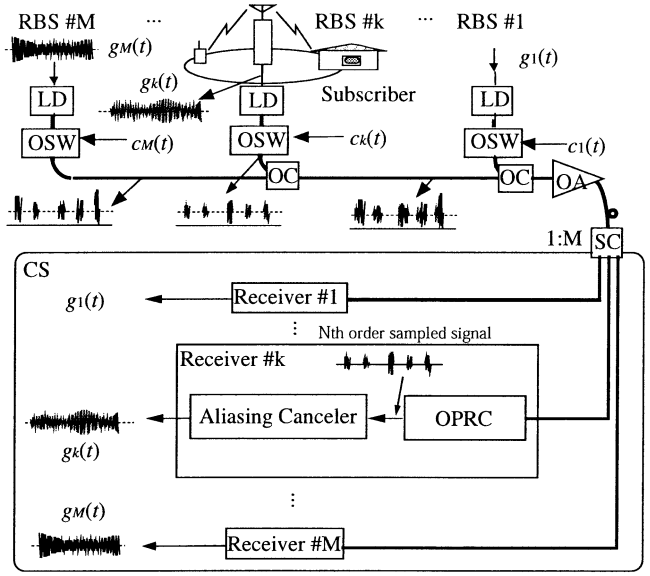

Fig. 8 Configuration of higher-order spread spectrum DOS-CDMA system.

3.3 System Configuration with Grouping Scheme

When DOS-CDMA system uses spreading codes each of which has n_p weight, "1," and also has the average pulse interval of less than T_S, n_pth order spectrum spreading can be applied. In this case, the aliasing canceler should be composed by a switch splitting n_p sampled pulses and n_p filters with appropriate transfer characteristics derived. But the derivation of $H_i(f)$ $(i = 1, 2, \cdots, n_p)$ is very complicated and it seems to be too difficult to realize. So we introduce a grouping scheme to make the receiver configuration simpler. Figure 9 illustrates the configuration example of the receiver using the grouping scheme. In the grouping scheme, we divide DOS-CDMA signal pulses into A groups including N pulses. For example, if DOS-CDMA signal is encoded by a code with n_p of 63, it is divided into 21 sets each of which has 3 pulses. In this case, the receiver can be constructed with 21 aliasing cancelers each of which is 3rd order aliasing canceler. Therefore, the derivation complexity of $H_i(f)$ can be extensively reduced from 63rd order to 3rd order, while the total number of BPF is still 63.

In the following description, we describe the grouping scheme for unipolar codes and bipolar codes.

3.3.1 Unipolar Codes

If we use unipolar codes such as prime codes as the spreading code of DOS-CDMA system, we can configure the receiver with a single OSW and a single PD [10]. The code length of prime codes is given by

$$L = p^2 \tag{17}$$

where p is a prime number. The grouping for prime codes is illustrated in Fig. 10(a). For example, if we apply 5th order bandpass sampling to a prime code with

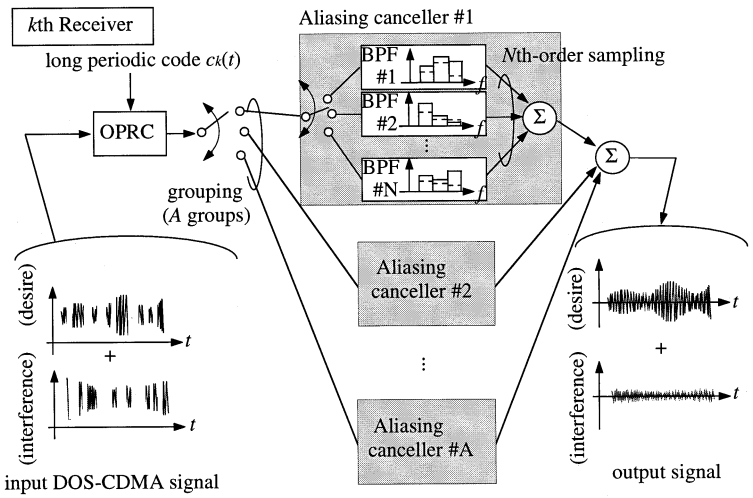

Fig. 9 Configuration of the receiver in grouping scheme.

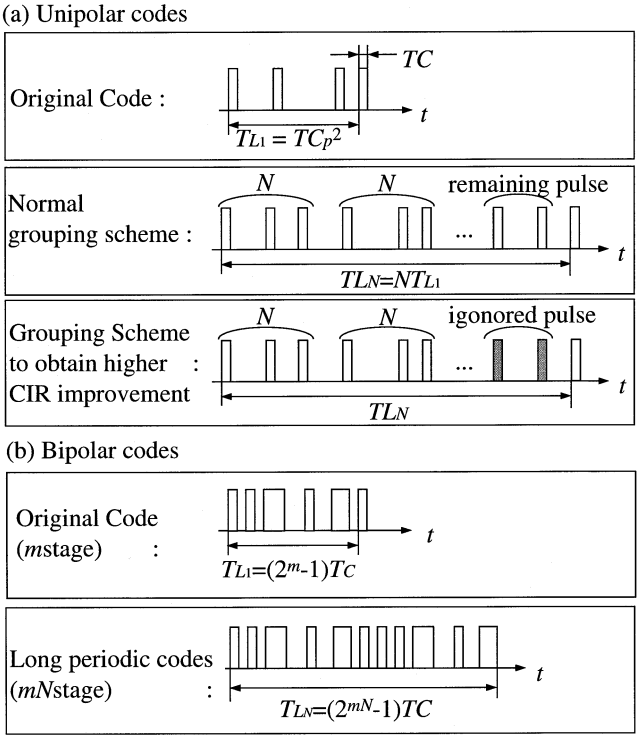

Fig. 10 Grouping scheme of spreading codes.

its p of 67, these code pulses are divided into groups of $(5, 5, \cdots, 5, 4, 4, 4)$. In this case, CIR improvement is dominated by the 4th order bandpass sampling.

So we consider the following grouping scheme, which makes as many groups including N pulses as possible, and ignores remaining pulses. As an example, in the case of length of 67^2, if we apply 5th order bandpass sampling to this code, these code pulses are divided into $(5, 5, 5, \cdots, 5, 2)$ and the last two pulses are ignored. This scheme is effective to obtain higher CIR improvement, however, when the code length is short, the power loss of code pulses deteriorates carrier-to-noise-power ratio (CNR).

3.3.2 Bipolar Codes

Figure 10(b) illustrates the grouping scheme for bipolar codes such as M sequences, Gold sequences and so on. For the bipolar codes, it is possible to divide code pulses into some groups without any remaining pulses. For example, in the case that 4th order bandpass sampling is applied to length of 63 code which has 32 of n_p, we can divide these pulses into $(4, 4, \cdots, 4)$.

But the following problem occurs in bipolar code. Code length of bipolar codes is given by

$$L = 2^m - 1 \tag{18}$$

where m is the number of shift-registers. When Nth order bandpass sampling is applied, code length, L_N, is expected to be

$$L_N = N \times L_1 \tag{19}$$

where L_1 is code length for 1st order bandpass sampling, that is, bandpass sampling. However, expanded code length is also required to be $2^m - 1$. Therefore expanded code length actually given is shorter than Eq. (19).

4. Theoretical Analysis of Signal Quality

4.1 Theoretical Analysis of CIR

We have explained that spectral aliasings in higher-order bandpass sampling are removed by the aliasing canceler proposed in Sect. 3.1. In the proposed system, desired signal and interference signals are passed through the aliasing canceler, however, we have described only the operation for the desired signal component in Sect. 3.1. So in this section, we describe the operation of aliasing canceler for the interference components and then analyze the CIR performance.

In the case of using M sequences as biased bipolar code, $c_k(t)$, for the Nth order bandpass sampling, $c_k(t)$ is written by

$$c_k(t) = \sum_{n=-\infty}^{+\infty} \sum_{i=1}^{L} \{p(t - iT_c - nT_{L_N}) \cdot d_{k_i}\} \tag{20}$$

where $d_{k_i} (= \{0, 1\})$ is the i-th chip of code sequence of k-th RBS. In the Nth order spread spectrum DOS-CDMA system, the desired component and interference components at the output of PD, $s_k(t)$ and $i(t)$, can be written by

$$s_k(t) = \alpha P_r^k g_k(t) \sum_{n=-\infty}^{+\infty} \sum_{i=1}^{L} \{p(t - iT_c - nT_{L_N}) \cdot d_{k_i}\} \tag{21}$$

and

$$i(t) = \sum_{l=1, l\neq k}^{M} \left[\alpha P_r^l g_l(t) \sum_{n=-\infty}^{+\infty} \sum_{i=1}^{L} \{p(t - iT_c - nT_{L_N}) \cdot d_{l_i}\} \times \sum_{n=-\infty}^{+\infty} \sum_{i=1}^{L} \{p(t - iT_c - nT_{L_N}) \cdot d_{k_i}\} \right] \tag{22}$$

where α, P_r^k and $g_k(t)$ are the responsivity of PD, the received optical signal peak power of k-th RBS, and the RF signal of the k-th RBS, respectively. Thus, their spectrum $S_k(f)$ and $I(f)$ are given by

$$S_k(f) = \alpha P_r^k \sum_{n=-\infty}^{+\infty} \sum_{i=1}^{L} \left\{ \frac{T_c}{T_{L_N}} \mathrm{sinc}\left(\frac{\pi n T_c}{T_{L_N}}\right) \cdot G_k\left(f - \frac{n}{T_{L_N}}\right) e^{j2\pi(iT_c)/T_{L_N}} \cdot d_{k_i} \right\} \tag{23}$$

and

$$I(f)=\sum_{l=1,l\neq k}^{M}\left[\alpha P_r^l\sum_{n=-\infty}^{+\infty}\sum_{i=1}^{L}\left\{\frac{T_c}{T_{L_N}}\mathrm{sinc}\left(\frac{\pi nT_c}{T_{L_N}}\right)\cdot G_k\left(f-\frac{n}{T_{L_N}}\right)e^{j2\pi(iT_c)/T_{L_N}}\cdot d_{l_i}\right\}\otimes\sum_{n=-\infty}^{+\infty}\sum_{i=1}^{L}\left\{\frac{T_c}{T_{L_N}}\mathrm{sinc}\left(\frac{\pi nT_c}{T_{L_N}}\right)e^{j2\pi(iT_c)/T_{L_N}}\cdot b_{k_i}\right\}\right] \tag{24}$$

where $G_k(f)$ is the spectrum of $g_k(t)$.

In the following analysis, we consider that the input pulses are divided into A groups each of which includes N pulses, and they are passed through the aliasing canceler for the Nth order bandpass sampling.

The b-th pulse in the a-th group, $f_{a,b}(t)$, is represented as

$$f_{a,b}(t)=\alpha P_r^k g_k(t)\cdot\sum_{n=-\infty}^{+\infty}p(t-((a-1)N+b)T_c-nT_{L_N})+i_{a,b}(t)\quad(a=1,2,\cdots,A:b=1,2,\cdots,N) \tag{25}$$

where $i_{a,b}(t)$ are given by

$$i_{a,b}(t)=\sum_{l=1,l\neq k}^{M}\left[\alpha P_r^l g_l(t)\sum_{n=-\infty}^{+\infty}\{p(t-((a-1)N+b)T_c-nT_{L_N})\cdot d_{l_{a,b}}\}\times\sum_{n=-\infty}^{+\infty}\{p(t-((a-1)N+b)T_c-nT_{L_N})\}\right] \tag{26}$$

Thus $F_{a,b}(f)$, the spectrum of $f_{a,b}(t)$ is written by

$$F_{a,b}(f)=\alpha P_r^k\sum_{n=-\infty}^{+\infty}\left\{\frac{T_c}{T_{L_N}}\mathrm{sinc}\left(\frac{\pi nT_c}{T_{L_N}}\right)G_k\left(f-\frac{n}{T_{L_N}}\right)\cdot e^{j2\pi(((a-1)N+b)T_c)/T_{L_N}}\right\}+I_{a,b}(f) \tag{27}$$

where $I_{a,b}(f)$ represents the spectrum of $i_{a,b}(t)$.

From Eq. (7), the output of the aliasing canceler, $S(f)$, is given by

$$S(f)=\sum_{a=1}^{A}(\sum_{b=1}^{N}H_{a,b}(f)F_{a,b}(f)) \tag{28}$$

The aliasing canceler output of each group is combined with each other after passed through the aliasing canceler, therefore, $S(f)$ can be written by

$$S(f)=A\times\sum_{b=1}^{N}H_b(f)F_b(f) \tag{29}$$

where $H_b(f)$ $(b=1,2,\cdots,N)$ represent the transfer function of filters consisting aliasing canceler for Nth order bandpass sampling.

The $S(f)$ includes the desired component, $S_D(f)$, and the interference component, $S_I(f)$. From Eq. (7), the spectrum of the aliasing canceler output of the desired signal, $S_D(f)$, is given by

$$S_D(f)=\alpha P_r^k\cdot 2B_{rf}T_CNG_k(f) \tag{30}$$

Thus, the carrier power C is given by

$$C=(\alpha P_r)^2\cdot 2AB_{rf}T_C \tag{31}$$

where P_r is the received optical peak power.

On the other hand, the output of the aliasing canceler for the interference signals, $S_I(f)$, becomes

$$S_I(f)=A\sum_{b=1}^{N}H_b(f)I_b(f) \tag{32}$$

Average interference power is

$$I=\frac{L_N-1}{2L_N}(M-1)\frac{(\alpha P_r)^2}{AN}2AB_{rf}T_C \tag{33}$$

where M is the number of connected RBSs. Let L'_N denotes the code length in grouping scheme. Thus, the received CIR for M sequences is given by

$$CIR_{N(M)}=\frac{2L_NAN}{(L_N-1)(M-1)}=\frac{L_NL'_N}{(L_N-1)(M-1)}\simeq\frac{L'_N}{(M-1)}\quad\text{for M sequences} \tag{34}$$

By using grouping scheme, some pulses in a code word are ignored. So L'_N is smaller than L_N, that is, $L'_N\leq L_N$.

By using similar derivation, received CIRs for other codes are theoretically derived as

$$\begin{cases}CIR_{N(p)}=\dfrac{L'_N}{0.29(M-1)}\quad\text{for prime codes}\\ CIR_{N(Gold)}=\dfrac{4}{M-1}\cdot\dfrac{L'_N(L'_N+1)^2}{L'^2_N+5L'_N+7}\quad\text{for Gold codes}\end{cases} \tag{35}$$

It is found from Eqs. (34), and (35) that the received CIR of the Nth order spread spectrum DOS-CDMA system using grouping scheme is given by replacing L of conventional DOS-CDMA system described in Eq. (2) with L'_N. This fact means that the interference power of the aliasing canceler output is equal to input power within the signal frequency band.

4.2 Numerical Results

In this subsection, some numerical results of CIR are

Table 1 Simulation forewords.

number of connected RBSs (M)	10
Responsivity of PD	0.8 A/W
PSD of relative intensity noise	−152 dB/Hz
Received optical signal peak power (P_r)	−10 dBm
Noise temperature	300 K
Load resistance	50 Ω
Carrier frequency of RF signal (f_0)	1.9 GHz
Bandwidth of RF signal (B_{rf})	300 KHz

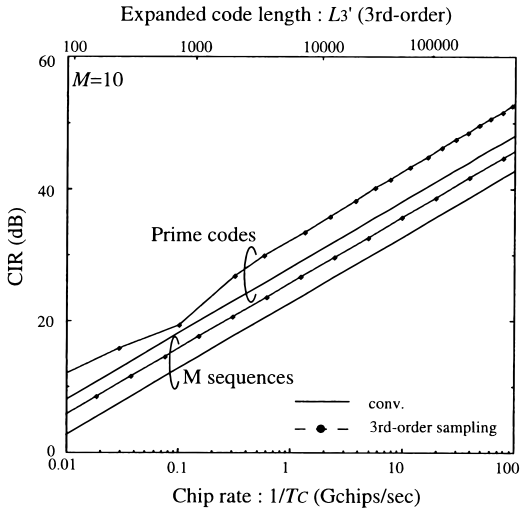

Fig. 11 Relationship between received CIR and chip rate, $1/T_C$.

shown and discussed. The parameters used for calculation are shown in Table 1. The number of connected RBSs, M, is 10 and received optical signal peak power, P_r, is −10 dBm, and carrier frequency of radio, f_0, and bandwidth of radio, B_{rf}, are 1.9 GHz and 300 kHz, respectively.

Figure 11 illustrates a relationship between the received CIR and the chip rate, $1/T_C$, which is the switching speed of OSW. It is found from this figure that the 3rd order spread spectrum DOS-CDMA system using grouping scheme can improve CIR by 5 dB compared with conventional 1st order bandpass sampling scheme for any codes, and CIR of prime codes is 5 dB better than that of M sequences, since the cross correlation value of prime codes is better than that of M sequences. Moreover, it is also found from this figure that to obtain the same CIR the 3rd order spread spectrum DOS-CDMA system using grouping scheme can reduce the chip rate to 1/3 value.

Figure 12 shows a relationship between the order of bandpass sampling and the CIR improvement for prime codes. At the high chip rate of 1 Gchips/sec, the CIR improvement of the proposed system closes to the upper bound derived in Sect. 2.2.2. On the other hand, at the low chip rate of 100 Mchips/sec, the CIR improvement varies according to the order of bandpass sampling. This is because the ignored code pulse in

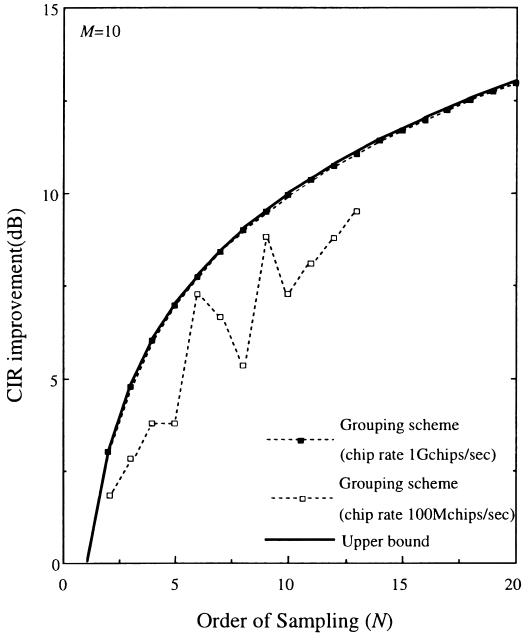

Fig. 12 CIR improvement in prime codes.

Table 2 Possible code length and the order of bandpass sampling for prime codes.

Order	100 Mchips/sec		1 Gchips/sec	
	Length (chips)	Group	Length (chips)	Group
2	17^2	2×8	53^2	2×26
3	19^2	3×6	67^2	3×32
.	.	.	.	.
13	43^2	13×3	141^2	13×10
.			.	.
20			179^2	20×16

grouping scheme is relatively large at the 100 MHz chip rate, thus this results in the variation of CIR. We show the set of possible code length and the components of groups which correspond to the code length actually used in Table 2.

Figure 13 shows a relationship between the order of bandpass sampling and the CIR improvement for M sequences. It is found that the CIR is improved similarly in both chip rates of 19 Mchips/sec and 1.23 Gchips/sec. Thus, in the M sequences, the influence of ignored pulses in the grouping is very small. This is because code lengths of M sequences are lengthened twice, and the CIR is improved per 3 dB. We also summarize the set of possible code length and components of groups in Table 3.

4.3 Theoretical Analysis of CINR

In the Nth order spread spectrum DOS-CDMA system using grouping scheme, the received noise power, P_N, is given by [9], [10]

$$P_N = P_{N_{\mathrm{RIN}}} + P_{N_{\mathrm{shot}}} + P_{N\mathrm{th}} + P_{N_{\mathrm{s-sp}}} + P_{N_{\mathrm{sp-sp}}} \quad (36)$$

where $P_{N_{\mathrm{RIN}}}$ represents the power of relative intensity

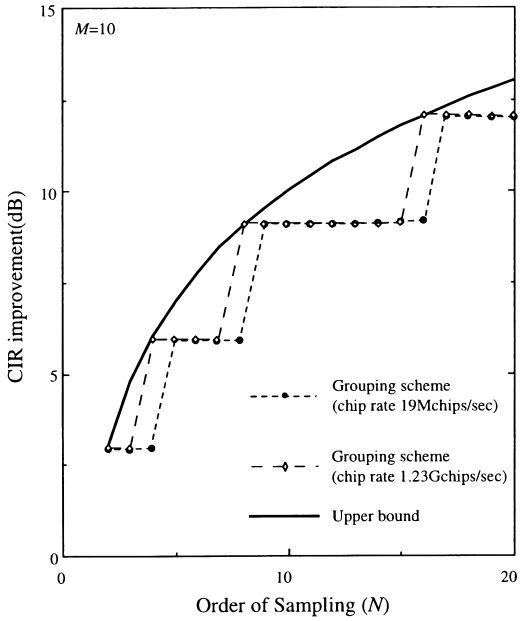

Fig. 13 CIR improvement in M sequences.

Table 3 Possible code length and order of bandpass sampling for M sequences.

Order	19 Mchips/sec		1.23 Gchips/sec	
	Length (chips)	Group	Length (chips)	Group
2	63	2×16	4095	2×1024
3	63	3×10	4095	3×682
.	.	.	.	.
8	127	8×8	16383	8×1024
.	.	.	.	.
20	511	20×12	32767	20×819

noise, $P_{N_{\rm shot}}$ represents the power of shot noise, $P_{N\rm th}$ represents the power of thermal noise, $P_{N_{\rm s-sp}}$ represents the power of beat noise between optical signal and spontaneous emission, and $P_{N_{\rm sp-sp}}$ represents the power of beat noise between spontaneous emissions, respectively. Their noise powers for M sequences are given by [9]

$$P_{N_{\rm RIN}} = n_{\rm RIN}\left(\frac{\alpha P_r}{L'_N}\right)^2\left[\left(\frac{L'_N+1}{2}\right)^2+(M+1)\cdot\left\{\left(\frac{(L'_N+1)^2}{4L'_N}\right)^2+\frac{(L'^2_N-1)^2}{4L'_N}\right\}\right]B_{rf}$$

$$P_{N_{\rm shot}} = 2e\left\{\left(\frac{\alpha P_r}{L'_N}\right)\frac{M(L'_N+1)}{2}+\alpha M(N_{sp}+N_{spM})W\right\}B_{rf}$$

$$P_{N\rm th} = 8k_BT_\theta B_{rf}/R_L$$

$$P_{N_{\rm s-sp}} = 4\alpha\left(\frac{\alpha P_r}{L'_N}\right)\frac{M(L'_N+1)}{2}\cdot M(N_{sp}+N_{spM})B_{rf}$$

$$P_{\rm sp-sp} = 2\alpha^2M^2(PN_{sp}+PN_{spM})^2(W-f_{rf}) \tag{37}$$

where $n_{\rm RIN}$, e, W, k_B, T_θ and R_L are the power spectrum density (PSD) of the relative intensity noise, the electric charge, the bandwidth of optical filter at the CS, Boltzman constant, the noise temperature and the load resistance, respectively. The PSD of the amplified spontaneous emissions, P_{sp} and P_{spM}, are given by

$$P_{sp} = \frac{\eta_{sp}}{\eta_a}\cdot\frac{10^{G/10}-1}{10^{G/10}}h_\nu$$

$$P_{spM} = \frac{\eta_{sp}}{\eta_a}\cdot\frac{M-1}{M}h_\nu \tag{38}$$

where η_{sp}, η_{spM} and h_ν are the spontaneous emission factor, the quantum efficiency of the OA and the photon energy, respectively. Similarly, a result of Eq. (36) can be referred for other codes.

From Eqs. (31), (33) and (36), CINR for Nth order spread spectrum DOS-CDMA system is given by

$$CINR_N = \frac{C}{I+P_N}. \tag{39}$$

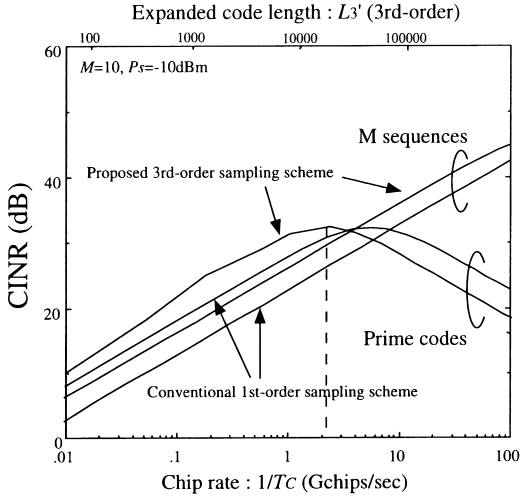

Fig. 14 Relationship between received CINR and chip rate, $1/T_C$.

4.4 Numerical Results of CINR

Figure 14 shows a relationship between CINR of the regenerated radio signals and chip rate. For the prime code, CINR of the 3rd order spread spectrum DOS-CDMA system using grouping scheme is maximized at about 2 Gchips/sec. Because its pulse duty decreases as the code length increases, therefore the RF carrier power is reduced. Hence, CINR for the higher than 2 Gchips/sec dominated by noises is deteriorated as the

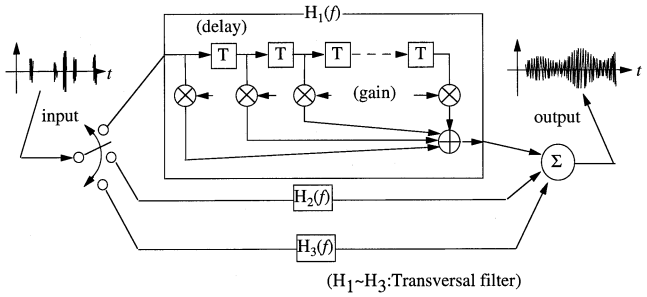

Fig. 15 Aliasing canceler constructed by transversal filters.

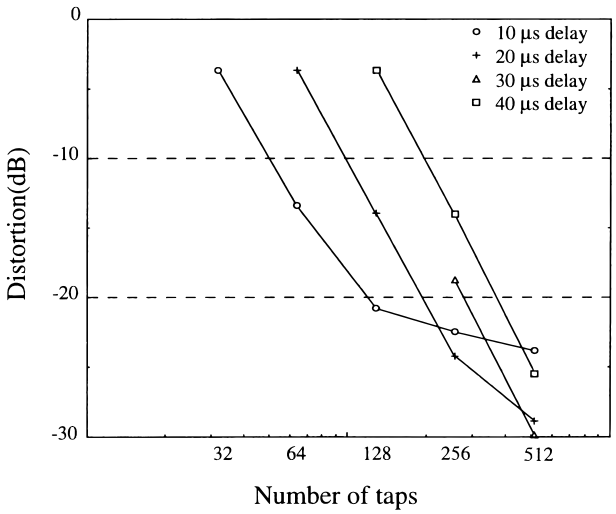

Fig. 16 Distortion of aliasing canceler constructed by transversal filters.

chip rate increases.

For the case of M sequences, on the other hand, the received CINR is improved as chip rate increases. This is because its pulse duty does not change as the code length increases. However, at the higher chip rate, the received CINR will be dominated by the additive noise, and it will reach to an upper bound.

5. Aliasing Canceler Composed by Transversal Filters

In the previous analyses, we assume an ideal aliasing canceler. So we construct the aliasing canceler by the use of transversal filters as shown in Fig. 15 and examine its performance. By using transversal filters, we can construct the aliasing canceler easily. The amplitude characteristics are controlled with the tap gain of transversal filters and the phase characteristics are controlled with the tap delay of transversal filters.

To estimate the distortion, we show the result of the computer simulations in Fig. 16. In this figure, we estimate the distortion by the mean square error of the variations between received RF signal and interpolated RF signal. We assume that the BPSK signal has a nyquist baseband waveform with its roll-off factor of 0.5, and its carrier frequency and bandwidth are 1.9 GHz and 300 kHz, respectively. This RF signal is 3rd order sampled and interpolated by the aliasing canceler constructed with transversal filters. It is seen from Fig. 16 that at least 128 taps of transversal filters with its unit delay of 10 μs are needed to reduce the distortion to -20 dB. The delay in this figure means the whole delay of the transversal filters, that is, the product number of taps and T shown in Fig. 15.

6. Conclusion

In this paper, we have proposed the higher-order spread spectrum direct optical switching CDMA system and an aliasing canceler. As results of theoretical examination of the signal quality, followings are found:
(1) The proposed 3rd order spread spectrum DOS-CDMA system using grouping scheme with an aliasing canceler can improve the CIR by 5 dB.
(2) As the result of the received CINR analysis, it is found that CINR of prime code has the optimum value and that of M sequences is improved while it is dominated by the additive noise.
(3) If we require -20 dB of distortion, at least 128 taps and 10 μs delay transversal filters are needed for 3rd-order bandpass sampling scheme.

As future study, we will investigate the general configuration of aliasing canceler constructed by transversal filters in Nth order, and we will evaluate the relationship between its distortion and the order of bandpass sampling.

References

[1] S.Komaki, K.Tsukamoto, M.Okada, and H.Harada, "Proposal of radio highway networks for future multimedia-personal wireless communications," ICPWC'94, pp.204–208, Bangalore, India, Aug. 1994.
[2] D.C. Cox, "A radio system proposal for widespread low-power tetherless communications," IEEE TRANS., vol.39, no.2, pp.324–335, Feb. 1991.
[3] H. Harada, S. Kajiya, K. Tsukamoto, S. Komaki, and N. Morinaga, "TDM intercell connection fiber-optic bus link for personal radio communication systems," IEICE Trans. Commun., vol.E78-B, no.9, pp.1287–1294, Sept. 1995.
[4] M.M. Banet and M. Kavehrad, "Reduction of optical beat interference in SCM/WDM networks using pseudorandom phase modulation," IEEE J. Lightwave Technol., vol.LT-12, no.10, pp.1863–1868, Oct. 1994.
[5] S. Kajiya, K. Tsukamoto, and S. Komaki, "Proposal of fiber-optic radio highway networks using CDMA method," IEICE Trans. Electron., vol.E79-C, no.1, pp.111–117, Jan. 1996.
[6] P.R. Prucal, M.A. Santoro, and T.R. Fan, "Spread spectrum fiber optic local area network using optical processing," IEEE J. Lightwave Technol., vol.LT-4, no.5, pp.547–554, May 1986.
[7] D. Zaccarin and M. Kavehrad, "All optical CDMA system based on spectral encoding of LED," IEEE Photon. Technol. Lett., vol.4, no.4, pp.479–482, April 1993.
[8] J.A.Salehi, A.M. Weiner, and J.P. Heritage, "Coherent ul-

trashot light pulse code-division multiple access communication systems," IEEE J. Lightwave Technol., vol.7, no.3, pp.478–491, March 1990.
[9] S. Park, K. Tsukamoto, and S. Komaki, "Polarity-reversing type photonic receiving scheme for optical CDMA signal in radio highway," IEICE Trans. Electron., vol.E81-C, no.3, pp.462–467, March 1998.
[10] S. Park, K. Tsukamoto, and S. Komaki, "Proposal of direct switching CDMA for cable-to-the-air system and its performance analysis," IEICE Trans. Commun., vol.E81-B, no.6, pp.1188–1196, June 1998.
[11] A. Kohlenberg, "Exact interpolation of band—Limited functions," J. Appl. Phys., vol.24, pp.1432–1436, Dec. 1953.
[12] K. Kumamoto, S. Park, K. Tsukamoto, and S. Komaki, "Higher-order bandpass sampling spreading scheme for direct optical switching CDMA radio highway," Proc. CPT'99, pp.111–112, Jan. 1999.
[13] K. Kumamoto, S. Park, K. Tsukamoto, and S. Komaki, "Application of aliasing cancelling scheme for direct optical switching CDMA system with higher-order bandpass sampling," Proc. PIMRC'99, no.A4-5, Sept. 1999.

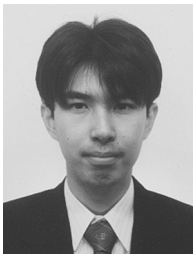

Kazuo Kumamoto was born in Hiroshima, Japan, on February 17, 1976. He received the B.E. and M.E. degrees in Communications Engineering from Osaka University, Osaka, Japan, in 1998 and 1999 respectively. He is currently pursuing the Ph.D. degree at Osaka University. He is engaging in the research on radio and optical communication systems.

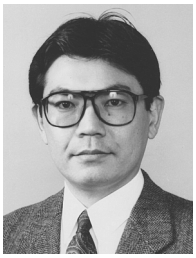

Katsutoshi Tsukamoto was born in Shiga, Japan in October 7, 1959. He received B.E., M.E. and Ph.D. degrees in Communication Engineering from Osaka University, Oska, Japan, in 1982, 1984 and 1995 respectively. He is currently an Associate Professor in the Department of Communications Engineering at Osaka University, and engaging in the research on radio and optical communication systems. He is a member of IEEE.

Shozo Komaki was born in Osaka, Japan in 1947. He received B.E., M.E. and Ph.D. degrees in Communication Engineering from Osaka University, Osaka, Japan, in 1970, 1972 and 1983 respectively. In 1972, he joined the NTT Radio Communication Labs., where he has engaged in repeater development for a 20-GHz digital radio system, 16-QAM and 256-QAM systems. From 1990, he moved to Osaka University, Faculty of Engineering, and engaging in the research on radio and optical communication systems. He is currently a Professor of Osaka University. Dr. Komaki is a senior member of IEEE, and a member of the Institute of Television Engineering of Japan (ITE). He was awarded the Paper Award and the Achievement Award of IEICE, Japan in 1977 and 1994 respectively.